

CRITICAL DISPLACEMENT PARAMETERS OF A TURBULENT BOUNDARY LAYER

V. M. Eroshenko, A. L. Ermakov,
A. A. Klimov, V. P. Motulevich,
and Yu. N. Terent'ev

UDC 532.526.4

The interferometer method was used for determining the critical displacement parameters of a turbulent diffusion boundary layer at a porous plate with injection of helium, nitrogen, carbon dioxide, krypton, xenon, and Freon-12. Velocity and concentration profiles were obtained for the critical flow modes.

In engineering practice it is very often necessary to protect surfaces against various detrimental effects of a gasodynamic stream: heating, corrosion, erosion, etc. The method of protection by a transverse feed of a fluid through permeable surfaces into the boundary layer is in this case very effective.

A surface is protected against the destructive effect of an external stream most effectively and also most economically by a critical mode of injection. This mode prevails [1, 2] when interaction between the mainstream and the surface begins to cease: $C_f/2 = St = St^* = 0$.

The conditions for a critical mode of injection are established, in terms of the asymptotic theory, on the basis of a model of a fluid flow with zero viscosity, i.e., with $Re \rightarrow \infty$ [1, 2]. When applied to a real flow with a finite Reynolds number, however, the theoretical values of the critical injection parameters require empirical corrections [2].

Attempts to experimentally determine the critical injection parameters under the simplest flow conditions ($Ma_0 = 0$, $dp/dx = 0$, $T_w/T_0 = 1$, $m_0/m_1 = 1$) were made a rather long time ago [3, 4]. Nevertheless, only a few studies on this subject have followed since. The values of b_{CR} published by various authors differ by as much as a factor of 3. No study of heterogeneous critical injection can be found in the available literature at all.

This situation has not come about accidentally. The crux of the matter is that the errors in the measurement of extremely small friction forces and thermal fluxes by conventional methods (thermocouples, Pitot tubes, thermoanemometer, Stanton tubes, floating probes) increase considerably under high injection rates. For this reason, in earlier studies [3, 4] the displacement parameters were determined in a rather qualitative manner and the subsequent quantitative generalizations were indicative of the author's viewpoint on the controversial subject concerning the finiteness of b_{CR} .

Data pertaining to the critical injection parameters of a subsonic turbulent boundary layer at a plate have been extracted from the technical literature and are shown in Fig. 1a. The dashed line here indicates the theoretical value of the displacement parameter with a correction for the finiteness of the Reynolds number [2]. The test data were obtained with a modified Stanton tube (point 1), by interferometry (2), by the transformed momentum equation and from velocity profile measurements (3-5), with thermocouples (6), and with chemical tracers (7).

The question about the finiteness of b_{CR} [1, 2] is important in principle. It is of rather academic interest, in our opinion, unless the stream pattern would be distorted appreciably when the true parameter values close to the extreme values at $b \rightarrow \infty$ are replaced by these extreme values at a finite b_{CR} . An essentially analogous situation prevails when the finite thickness of the boundary layer is to be introduced into the analysis, but in practice, as is well known, that does not result in large errors.

Translated from *Inzhenerno-Fizicheskii Zhurnal*, Vol. 23, No. 1, pp. 94-103, July, 1972. Original article submitted October 12, 1971.

© 1974 Consultants Bureau, a division of Plenum Publishing Corporation, 227 West 17th Street, New York, N. Y. 10011. No part of this publication may be reproduced, stored in a retrieval system, or transmitted, in any form or by any means, electronic, mechanical, photocopying, microfilming, recording or otherwise, without written permission of the publisher. A copy of this article is available from the publisher for \$15.00.

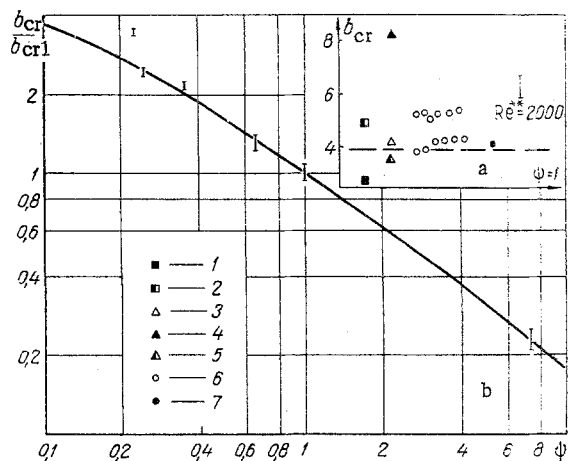


Fig. 1. Effect of the heterogeneity factor (ψ) on the critical injection parameter: data from [3, 4] (1), data from [5] (2), data from [6] (3, 4, 5), data from [7] (6), data from [8, 9] (7), data obtained in this study (I), results based on asymptotic theory [2] (curve).

In this study the authors have experimentally determined the critical displacement parameters of a diffusion boundary layer with various injected gases. The heterogeneity was varied over a wide range $\psi = m_o/m_i = 0.22-7.24$. The interferometric method of displacement study offered several advantages over other methods and actually yielded the answers to our problem. The main advantage of interferometry is that its accuracy does not become worse as the Stanton number St^* tends toward zero with an increasing injection rate (which was a serious obstacle to a reliable determination of b_{cr} in earlier attempts), and even improves somewhat because of smaller refractive errors. The determination of displacement parameters does not require a solution of equations idealizing the transfer processes (e.g., the momentum equation) nor a differentiation of empirical equations, which would lead to large errors. The value of b_{cr} is obtained directly from interferometric measurements, owing to the high sensitivity of this method.

The tests were performed in an aerodynamic tunnel operating continuously in the atmosphere-vacuum mode [10]. The apparatus was equipped with a lot of modern precision control-and-measuring instruments, including a model IT-14 Mach-Zender interferometer with laser sources [11] and a thermoanemometer by the DISA Co. (made in Denmark).

The test model was a 132×40 mm² plate of porous nickel mounted flush into the bottom wall of a square channel. The opposite channel wall was made of 2 mm thick flexible acrylic glass. It was supported on four micrometer screws, in order to make it possible to adjust the duct section and thus the pressure gradient in the outer stream.

For a more uniform distribution of the flow rate, the porous plate was made of four isolated from one another sections. The gas was injected from a high-pressure tank through a filter system and a flow metering segment to each plate section independently.

Prior to the main series of experiments, a few qualification tests had revealed a fully turbulent boundary layer along the entire plate - beginning at approximately 150 mm upstream beyond the porous insertion. The Reynolds number of the oncoming stream was $Re_x = 200,000$. The forerunning layer was not sucked out. Special tests showed, however, a rather fast readjustment of the flow pattern to conform to new boundary conditions. Thus, for instance, with an injection of gaseous carbon dioxide at a rate $F = 1.35\%$ ($b_L = 4.7$, subcritical mode), the similarity region of velocities and concentrations began already at a distance $x = 80-90$ mm. The length of the initial region decreased fast with higher injection rates.

An excellent uniformity and a low turbulence ($\epsilon = 0.13\%$) across the channel were ensured by honeycombing and converging.

Measurements of the velocity profiles and of the skin-friction coefficients indicated a smooth aerodynamic stream along the porous plate. Indeed, the test plate made of porous nickel by powder metallurgy processes had a fine grain structure (powder particles about $2 \mu m$ in diameter, dimension of pores about $8 \mu m$, porosity about 65-70%). Evidently, the roughness height of this plate was not more than $10 \mu m$, i.e., by one order of magnitude under the allowable roughness height according to [12].

For checking how uniform the permeability of the plate was, we used a miniature thermoanemometer tube and moved it around along the channel axis at a distance approximately 0.8 mm from the wall in a plane parallel to it. The standard deviation of the measured injection velocity over a length of approximately 35

mm at the plate edge was 10%. For calculating the injection parameter $F = (\rho v)_w / (\rho u)_0$, the flow intensity at the wall $(\rho v)_w$ was determined not from the local injection velocity but from the mean-rate velocity per unit model area.

As the acting gases we used helium, nitrogen, carbon dioxide, krypton, xenon, and Freon-12. Because of the small difference between the molal refraction of nitrogen and the molal refraction of the oncoming air stream, the interferometric method of determining the displacement parameters could not be used in this case. For this reason, with nitrogen injection, b_{cr} was determined from the velocity profile.

For fixed parameters of the oncoming stream, the displacement of the diffusion boundary layer depended on two factors: the injection rate F and the locality of the given section. The displacement parameter was defined as $b = F/X$ with $X = 0.296Re_x^{-0.2}$ ($Re_x = u_0 x / \nu_0$, and x measured from the injection starting point), which made it possible to compare our b_{cr} with the results of the asymptotic solution [2].

In order to obtain consistent test data, the displacement parameters of the diffusion boundary layer under injection of the various gases were measured at the end of the plate. In this way, b_{cr} was determined in our test by varying F . Because of the small plate dimensions, no attention was paid to the effect of length X on b_{cr} .

The critical injection parameters were determined as follows. The same constant velocity of the quiescent stream was established in each test. The respective gas was supplied from its high-pressure container to the model at such a flow rate as to ensure the prescribed subcritical flow mode along the entire porous surface. The mainstream velocity was measured with a thermoanemometer tube along the plate. With the aid of the flexible upper wall and by its proper positioning we established a zero-gradient flow (with 1-2% of the velocity). The interference pattern was then photographed on a large-size grade 17 aero-isopanchromatic film to a 1:1 scale and with an approximately $5 \cdot 10^{-8}$ sec exposure to a ruby-laser pulse of modulated quality.

Following this, the injection rate was increased in sufficiently small steps, with both the photographic and the flow adjustments repeated each time. Photography was continued until the displacement could be seen on the interferometer receiver screen with a naked eye.

The object was photographed with the interferometer set initially for vertical fringes of finite width. With such a setting, the mixing zone of both streams was indicated by a perturbation of interference fringes representing, to a certain scale, the profile of injected gas concentration.

The interferograms were examined under a model MMI-2 microscope with a $\times 50$ magnification. A displacement of the concentration boundary layer occurs when the Stanton diffusion number becomes equal to zero:

$$St^* = \frac{D_w \left(\frac{d\rho_1}{dy} \right)_w}{\Delta\rho_1 u_0} = 0. \quad (1)$$

At the given initial interferometer setting, therefore, a sweepoff was characterized by a perturbation of interference fringes perpendicular to the surface.

After each scanning of a series of interferograms, two consecutive frames were selected with no displacement yet seen on the first one and a displacement by a fraction of a millimeter already seen on the next one. Obviously, the injection parameter was critical within the preselected range of injection rates between the two consecutive interferogram frames. Subsequently, on account of the extent of the displacement region, the critical parameters are given in terms of the most likely intervals.

The asymptotic theory in [2] has yielded the limits of displacement parameter values:

$$\begin{aligned} \psi < 1; b_{cr} &= \frac{1}{1-\psi} \left(\ln \frac{1+\sqrt{1-\psi}}{1-\sqrt{1-\psi}} \right)^2, \\ \psi > 1; b_{cr} &= \frac{1}{\psi-1} \left(\arccos \frac{2-\psi}{\psi} \right)^2. \end{aligned} \quad (2)$$

The analytical formulas (2), which represent the functional relation $b_{cr} = f(\psi)$, have been obtained for $Re \rightarrow \infty$ and, therefore, yield absolute values of b_{cr} too low at a finite Reynolds number as it would be in a test. Consequently, experimental results are gaged against the theoretical relations as follows (Fig. 1b):

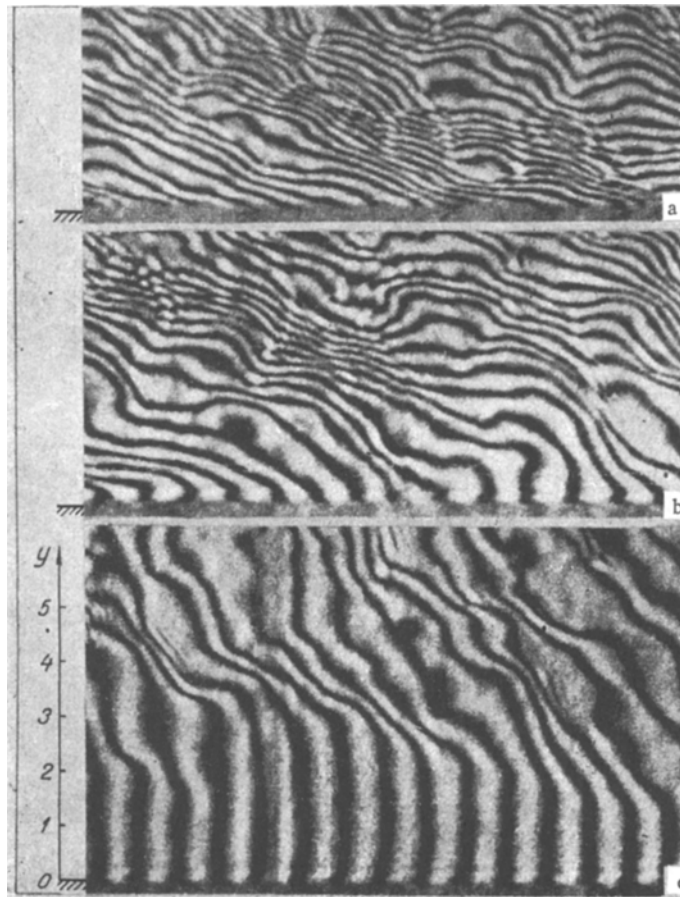


Fig. 2. Interferograms of the sublayer in a turbulent boundary layer under an increasing rate of Freon-12 injection. Ordinate y (mm).

TABLE 1. Displacement Parameters of a Diffusion Boundary Layer

Injected gas	Heterogeneity factor, ψ	Displacement parameter	Power exponent n
Helium	7,24	1,3—1,6	$n_r \approx 1,1 \div 1,4$ $n_m \approx 5,6$
Nitrogen	1,03	5,9—6,7	$n_u \approx 1,3$
Carbon dioxide	0,66	7,9—8,8	$n_r \approx 1,2 \div 1,4$ $n_m \approx 1,0 \div 1,2$ $n_u \approx 1,1 \div 1,2$
Krypton	0,34	13,1—14,0	$n_r = 1,3$ $n_m = 0,72$
Freon-12	0,24	14,7—15,2	$n_r \approx 1,4$ $n_m = 0,72$ $n_u = 0,72$
Xenon	0,22	21,0—21,8	$n_r \approx 1,5$ $n_m \approx 0,62$

$$\frac{b_{cr}}{b_{cr}|_{Re_x}} = f(\psi), \quad (3)$$

where b_{cr1} is the displacement parameter value at $\psi = 1$. According to Fig. 1b, the result of such a calibration is entirely satisfactory. An exception here is the injection test with xenon ($\psi = 0.22$). Because the injection time was short, on account of the high cost of this gas, it was not possible to quite eliminate the longitudinal pressure gradient in the outer stream. The disqualification of the value of b_{cr} for xenon from the generalizing curve does clearly illustrate how sensitive the critical displacement parameter is to negative pressure gradient in the outer stream.

We note that an increasing rate of transverse flow in the stream gives rise to a new effect, namely a negative pressure gradient, which affects the flow

dynamics. A negative pressure gradient in the interaction zone of both streams is caused by two factors: first of all, the displacing action of the injection zone in a potential flow and, secondly, the jumpwise discontinuance of injection behind the porous plate analogous to that noted in a sudden widening of the stream around a finite wedge.

Displacement of the mainstream by the boundary layer can be eliminated, for example, by means of the flexible upper channel wall. As to the second factor, namely the pressure field induced upstream by

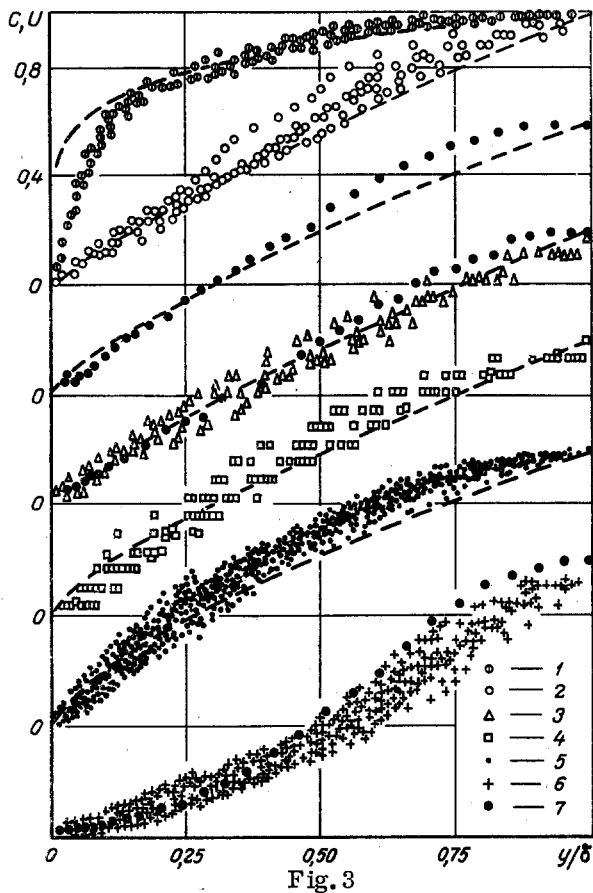


Fig. 3

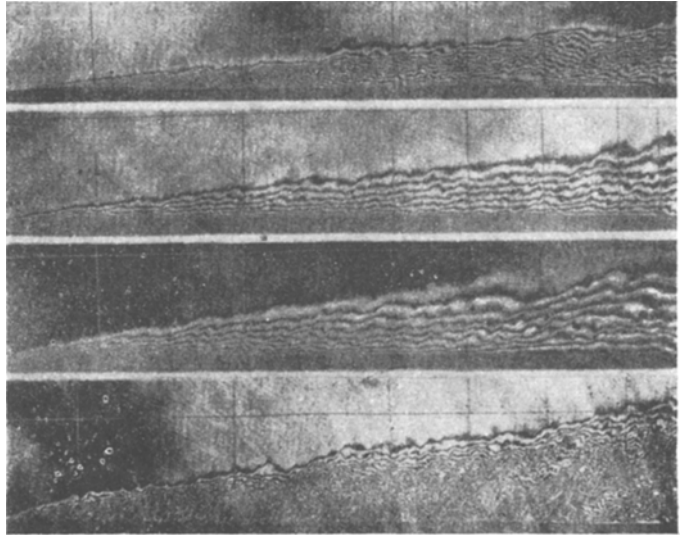


Fig. 4

Fig. 3. Dimensionless profiles of velocity (points 7), of mass concentration (1, 6), and of volume concentration (2, 3, 4, 5) at critical rates of helium, gaseous carbon dioxide, krypton, and Freon-12 injection. The dashed curves represent power-law profiles (see Table 1).

Fig. 4. Interferograms of a turbulent boundary layer at critical helium, gaseous carbon dioxide, krypton, and Freon-12 injection.

the discontinuance of injection, its scale depends on the thickness of the boundary layer near the end of injection. Since this thickness is proportional to the length of the porous plate, it is not possible to prevent the emergence of a negative pressure gradient by increasing the plate dimensions.

The tests with a high rate of helium injection have confirmed the presence of a negative pressure gradient in the displacement zone with a zero-gradient outer stream. In order to prove this, we measured the velocity profiles at $F = 0.72\%$ (supercritical injection). The velocity profiles thus obtained had a distinct peak within the displacement zone. As the injection rate was increased, the velocity peak also increased. A zero-gradient flow in an unperturbed stream was attained experimentally with the aid of the flexible upper wall.

We should refer to the fact that an analogous effect of a negative pressure gradient arising in a supersonic stream at a plate with a high rate of injection across its surface has been analyzed theoretically in [13].

The theoretical formulas (2) apply to the case where $dp/dx = 0$. It is quite probable that the absolute values of the displacement parameters were too low not only because the Reynolds number had been assumed infinite, but also because the pressure field induced under actual conditions has been disregarded.

Typical interferograms of a boundary layer segment under an increasing rate of gas injection are shown in Fig. 2a, b, c. The interferometer was initially set for vertical fringes of finite width. The interferograms here illustrate clearly the successive displacement stages in a diffusion boundary layer. The interference fringes in Fig. 2c are oriented at right angles to the surface and the zone of constant concentration, i. e., the displacement zone has an easily measured finite thickness. The pattern indicates the obvious possibility of sweeping off the concentration layer.

In the earlier study [4] dealing with the effect of air or carbon dioxide injection on the average velocity and concentration profiles, qualitative conclusions were drawn concerning the subsequent distortion of these profiles. An analysis of the test data has shown that, as the injection rate increases, velocity and concentration profiles become distorted in three successive stages. It is noteworthy that the profile which prevails between the first and the third stage (boundary-layer profile and jet profile respectively) is characterized by a constant gradient of whatever measured quantity throughout about 70-80% of the boundary-layer thickness (linear profile).

Dimensionless profiles of velocity and injected gas concentration are shown in Fig. 3 for near-critical injection of various gases. It is evident that some of the profiles have one common feature: they are almost linear. Thus, the second stage of profile distortion corresponds to the beginning of displacement and, consequently, the shape of a profile indicates the flow mode (subcritical, critical, or supercritical). This fact was utilized in determining b_{cr} for nitrogen.

Interferograms of a turbulent boundary layer with critical injection of various gases are shown in Fig. 4. The initial interferometer setting was for an infinite fringe width. The diagram indicates that the thickness of an injection layer depends strongly on the kind of injected gas and is not just a simple function of the heterogeneity factor ψ .

Under definite flow conditions there is a relation between the processes of momentum, heat, and mass transfer which can be expressed by an analog of the Reynolds number: $c_f/2 = St = St^*$. Evidently, our data on critical injection parameters can be applied to heat transfer, inasmuch as the thermal boundary layer is as conservative with respect to various dynamic perturbations as the concentration boundary layer. As far as the hydrodynamic boundary layer is concerned, a negative pressure gradient arising under high injection rates can obviously cause displacement to occur either at somewhat higher values of the injection parameter or asymptotically. In practice, however, the displacement of a hydrodynamic boundary layer is not as important as the displacement of a thermal or a diffusion boundary layer.

NOTATION

x, y	are the longitudinal and transverse coordinate;
u, v	are the longitudinal and transverse velocity component;
ρ	is the density;
ρ_1	is the partial density;
D	is the diffusivity;
p	is the pressure;
m	is the molecular weight;
δ	is the layer thickness;
c	is the concentration;
ϵ	is the turbulence factor;
c_f	is the local skin-friction coefficient;
St	is the Stanton diffusion number;
Re, Re^*	are the Reynolds number based on geometrical dimensions;
Ma	is the Mach number;
$F = (\rho v)_w / (\rho u)_o$	is the injection parameter;
$\psi = m_o / m_i$	is the heterogeneity factor;
$b = F/X$	is the displacement parameter;
L	is the plate length;
r	is the volumetric;
m	is the mass;
u	is the velocity;
U, C	are the relative velocity and concentration.

Subscripts

o	denotes outer edge of boundary layer;
w	denotes wall;
i	denotes injected gas;
cr	denotes critical mode;
r	denotes volume.

LITERATURE CITED

1. S. S. Kutateladze and A. I. Leont'ev, Turbulent Boundary Layer of a Compressible Gas [in Russian], Izd. Sibirsk. Otdel. Akad. Nauk SSSR, Novosibirsk (1962).
2. S. S. Kutateladze, A. I. Leont'ev, et al., Heat and Mass Transfer and Friction in a Turbulent Boundary Layer [in Russian], Izd. Sibirsk. Otdel. Akad. Nauk SSSR, Novosibirsk (1964).
3. D. S. Hacker, R56AGT215, Cincinnati, Ohio (1956).
4. D. S. Hacker, Jet Propulsion, 26, No. 9 (1956).
5. D. S. Hacker, ASTE Paper NA-249 (1958).
6. E. Baker, Ph. D. Thesis, Imperial College of Science and Technology, Department of Mechanical Engineering, London (1967).
7. R. I. Moffat and W. M. Kays, Internatl. J. Heat and Mass Transfer, 11, No. 10 (1968).
8. A. I. Leont'ev, B. P. Mironov, and P. P. Lugovskoi, Inzh. Fiz. Zh., 10, No. 4 (1966).
9. S. S. Kutateladze, A. I. Leont'ev, and B. P. Mironov, in: Heat and Mass Transfer [in Russian], Izd. Nauka i Tekhnika, Minsk (1968), Vo. 1.
10. V. M. Eroshenko, M. G. Morozov, V. P. Motulevich, Yu. N. Petrov, and V. S. Pushkin, in: Physical Gasodynamics and Heat Transfer [in Russian], Izd. Akad. Nauk SSSR, Moscow (1961).
11. B. N. Baskarev, V. M. Eroshenko, A. A. Mushinskii, and Yu. N. Terent'ev, Inzh. Fiz. Zh., 17, No. 2 (1969).
12. G. Schlichting, Boundary-Layer Theory [Russian translation], Izd. Nauka, Moscow (1969).
13. F. L. Fernandez and L. Lis, Rocket Engineering and Cosmonautics, 8, No. 7 (1970).
14. V. M. Eroshenko, A. L. Ermakov, A. A. Klimov, V. P. Motulevich, and Yu. N. Terent'ev, Izv. Akad. Nauk SSSR, Mekhanika Zhidkosti i Gaza, No. 1 (1971).